A 60-GHz Optoelectronic Mixing Scheme of High Image and Carrier Rejection Ratios With an Integrated Optical Single-Sideband Modulator Employed

Yasuyuki Ozeki, *Student Member, IEEE*, Kaoru Higuma, Satoshi Oikawa, Masato Kishi, and Masahiro Tsuchiya, *Member, IEEE*

***Abstract*—We report on the first implementation and performance investigation of a 60-GHz-band optoelectronic image rejection mixing scheme based on a broad-band integrated optical single-sideband modulator. We have confirmed a few advantageous features over electrical image rejection mixers, arising from its nature of being free from electrical phase control of millimeter-wave signals. We obtained at the IF frequency of 800 MHz rejection ratios of $>$40 dB for the image signal and of $>$20 dB for the local oscillator (LO) signal in the LO frequency range of 55–65 GHz. The LO bandwidth can be extended further. The IF bandwidth with an image rejection ratio of $>$20 dB was also confirmed to be as broad as 550 MHz, which is limited not by the configuration but by the bandwidth of the 90° hybrid used in this experiment. Furthermore, fiber-optic transmission of a 155.52-Mb/s-DPSK 59.8-GHz optical millimeter-wave signal was successfully demonstrated for a 20-km standard single-mode fiber. A bit error rate of $<10^{-9}$ was achieved at the received optical power of -18 dBm with a negligible dispersion penalty.**

***Index Terms*—Fiber-optic millimeter-wave link, image rejection mixer, millimeter-wave mixer, optical single-sideband modulator, optoelectronic mixing.**

I. Introduction

THE millimeter-wave band has attracted considerable attention recently for its possible application to future broad-band multimedia access systems employing the picocell configuration. Since a large number of base stations are needed therein, the simplification of antenna base stations (BSs) is one of the key issues addressed for the cost reduction of system construction and maintenance. The schemes of fiber-optic millimeter-wave links [1]–[3] offer possible solutions for the BS simplification; one can generate a millimeter-wave signal at a central station (CS), transmit it to BSs via optical fibers, and centralize most of the millimeter-wave components into a CS such as local oscillators (LOs), mixers, and other signal processing functionalities. The simplification also leads to the implementation of highly transparent BSs, which are robust to the changes in the frequency and modulation formats. This feature is attractive especially in the millimeter-wave band, where a variety of wireless services will be brought into its unlicensed band of several gigahertz in the near future. Indeed, an extremely wide unlicensed band of 59–66 GHz has already been released in Japan [4]. Together with the reduction in numbers and costs of optical components, therefore, such BS simplification may accelerate the move to advanced millimeter-wave photonic systems.

One requirement will be to deal with various modulation formats and/or subcarrier multiplexing in such millimeter-wave photonic systems, where millimeter-wave radio frequency (RF) signals should be generated by upconversion of electrically processed signals of intermediate frequencies (IF). LOs and image components generated in the process of upconversion should be removed before the RF signal is emitted into the air from the viewpoint of efficient use of frequency resources. Such a signal rejection functionality is enabled by either of the following conventional methods: 1) the electrical filtering in BS or CS or 2) the use of a millimeter-wave band image rejection mixer in CS. Although the former eliminates the unnecessary signals with a high rejection ratio, the RF frequency will be fixed through the use of filters and the system transparency is degraded. Whereas the latter allows a variation in the RF frequency, millimeter-wave image rejection mixers (IRMs) of high rejection ratios are still under development, most likely due to the difficulty existing in the precise control of phases and amplitudes of millimeter-wave signals. Therefore, development of an image rejection mixing technique not only of a fiber-radio-compatible nature but also of higher performance in the millimeter-wave band is highly in demand so as to realize such advanced fiber-optic picocell downlinks with highly transparent BSs.

On the other hand, optoelectronic mixing techniques [5], [6] have been demonstrated for the fiber-optic millimeter-wave links in which upconverted signals are obtained through the external modulation of an optical LO signal by an electric IF signal or vice versa. One can see the following attractive features of

Manuscript received January 5, 2001; revised May 25, 2001. This work was supported by the programs of the Telecommunications Advancement Organization of Japan (TAO), by the Research for the Future Program of Japan Society for the Promotion of Science (JSPS), and by the Core Research for Evolutional Science and Technology (CREST) of the Japan Science and Technology Association (JST).

Y. Ozeki, M. Kishi, and M. Tsuchiya are with the Department of Electronic Engineering, University of Tokyo, Tokyo 113-8656, Japan (e-mail: ozeki@ktl.t.u-tokyo.ac.jp).

K. Higuma and S. Oikawa are with the New Technology Research Laboratories, Sumitomo Osaka Cement, Chiba 274-8601, Japan.

Publisher Item Identifier S 0018-9480(01)08721-X.

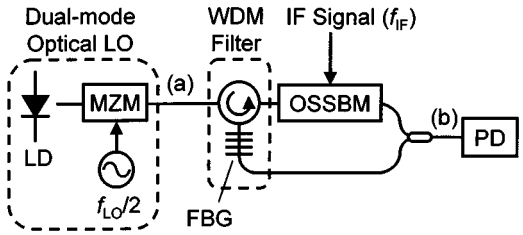

Fig. 1. Schematic of the OE-IRM configuration: (a) and (b) indicate the points corresponding to the optical spectra shown in Fig. 2.

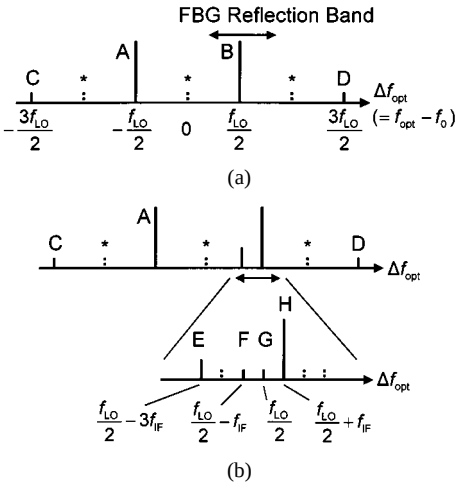

Fig. 2. Optical spectra of a dual-mode LO signal of (a) MZM output and (b) OE-IRM output. The horizontal axis shows the differential optical frequency $\Delta f_{\rm opt}$ from the LD light frequency f_0. Asterisks indicate the suppressed signal by the DSB-SC method. Symbols A–H are described in the text.

this: 1) no electrical signal processing in the millimeter-band is needed and 2) the mixed output is an optical signal and ready to be launched into a transmission fiber, which is suitable for the fiber-optic millimeter-wave links. However, their modulation formats have been so far fixed mostly to the amplitude or phase modulation of double sideband. Previously, we have introduced the concept of optoelectronic image and carrier rejections into optoelectronic mixing [7]. Its expected performance would even exceed that of an electrical IRM since it needs no phase or amplitude control of a millimeter-wave signal. The following is a summary of our work on the optoelectronic IRM (OE-IRM). First, the proposal and preliminary experiment were carried out on a primitive OE-IRM with an acoustooptic modulator utilized, resulting in both image rejection (IR) and LO rejection (LR) ratios of more than 36 dB, whereas the IF bandwidth was extremely narrow. It was followed by the OE-IRM proposal based on the polarization-mode dispersion (PMD) filtering method. A 20-dB IR ratio was derived over an IF band of $>$400 MHz around the IF center frequency of 2 GHz. Third, we successfully demonstrated the fiber-optic transmission of 155.52 Mb/s ASK and DPSK optical millimeter-wave signals over a 20-km standard single-mode fiber (SMF) [8], [19]. However, there are drawbacks left in the PMD filtering method; a delicate control of polarization states is inevitable and the IF bandwidth is still narrower compared to typical electrical IRMs.

In this paper, we report on the implementation and performance investigation of an improved OE-IRM scheme. The improvement was brought by a use of an integrated optical single-sideband modulator (OSSBM) [9], [10], with which the above problems of the PMD-based method were solved almost completely. In addition, we found out that the present scheme is superior to electrical IRMs; a fairly high IR ratio can be provided over a substantially wide LO frequency range. Furthermore, a successful demonstration was performed in a transmission experiment using a fiber-optic millimeter-wave downlink with the new OE-IRM scheme employed.

II. Principle of the OE-IRM Based on the Broad-Band Integrated OSSBM

Fig. 1(a) shows a schematic of the present OE-IRM configuration.[1] A dual-mode optical LO signal source is necessary and it is provided here by a Mach–Zehnder modulator driven by the method of double sideband modulation with the suppressed carrier (DSB-SC) [12]. Fig. 2(a) shows its schematically drawn optical spectrum. The optical carrier at f_0 and the even-order sidebands are suppressed and indicated by the asterisks in the figure. The first- and third-order sidebands are generated at $f_0 \pm f_{\rm LO}/2$ and $f_0 \pm 3f_{\rm LO}/2$, respectively, which are shown by A, B, C, and D. The latter two are negligibly small in the case of a low modulation index. Note that the DSB-SC method needs only an electric LO signal of $f_{\rm LO}/2$, as shown in Fig. 1. Other dual-mode optical sources [13]–[15] are also acceptable in this OE-IRM configuration, leading to the reduction of the driving frequency in any case.

One of the two modes is separated by a wavelength division multiplexing (WDM) splitter, which in this case consists of an optical circulator and a fiber Bragg grating (FBG) whose reflection band is adjusted so that the $f_0 + f_{\rm LO}/2$ mode [B in Fig. 2(a)], is included in it. Then the reflected mode is led into an OSSBM device, to which an electric IF signal is applied and whose detailed operation principles are available in [9]. The OSSBM output light, which we define as the optical IF signal hereafter, contains the optical upper-sideband (OUSB) at $f_0 + f_{\rm LO}/2 + f_{\rm IF}$ [shown by H in Fig. 2(b)] and some higher order components. The original mode at $f_0 + f_{\rm LO}/2$ and optical lower sideband (OLSB) at $f_0 + f_{\rm LO}/2 - f_{\rm IF}$ are suppressed sufficiently, which are defined as G and F in Fig. 2(b), respectively. We should note that the third-order lower sideband at $f_0 + f_{\rm LO}/2 - 3f_{\rm IF}$ [shown by E in Fig. 2(b)] is not negligible in the case of a high modulation index. By combining the FBG transmitted light and the optical IF signal, we obtain the OE-IRM output signal, and its spectrum is schematically shown in Fig. 2(b). Note that the signal is of optical single-sideband, providing the robustness to the chromatic dispersion penalty [16]. Photodetection of the OE-IRM output leads to sufficient generation of the upper sideband (USB) signal at $f_{\rm LO} + f_{\rm IF}$, while the lower sideband (LSB) signal at $f_{\rm LO} - f_{\rm IF}$ and the LO signal at $f_{\rm LO}$ are suppressed. Here, the third-order sideband at $f_{\rm LO} - 3f_{\rm IF}$ can be a dominant spurious component for an IF signal input of higher power. We define hereafter the IR ratio, the LR ratio, and the third-order sideband rejection (TR) ratio as the RF power suppression ratio of the LSB, the LO, and the

[1]A similar configuration has been proposed for different purposes from ours; for instance, see [11].

third-order sideband components to the USB component, respectively.

The LO and IF frequency responses predicted for this OE-IRM scheme are described below. The LO bandwidth depends in principle on the WDM filter characteristics and the spectral bandwidth of the OSSBM operation. The latter is less serious than the former and its broad-band nature is described in more detail in [17]. As for the former, one mode of the DSB-SC optical LO signal, which is allocated at $f_0 + f_{\rm LO}/2$ [B in Fig. 2(a)], should stay within the FBG reflection band. Therefore, the LO frequency is restricted in the range of $2(f_1 - f_0) - \delta f < f_{\rm LO} < 2(f_1 - f_0) + \delta f$, provided that the fluctuation in f_0 and f_1 is much less than δf, i.e., a few GHz, and that the FBG reflection band ranges from $f_1 - \delta f/2$ to $f_1 + \delta f/2$. Here, f_1 and δf are the center optical frequency and the bandwidth of FBG reflection, respectively. Such stability is available through the recent techniques for wavelength control and leads to the LO signal bandwidth of around $2\delta f$, i.e., twice as broad as the FBG reflection bandwidth. This is an attractive feature of the present OE-IRM scheme, while electrical IRMs, for which a precise phase control is unavoidable, cannot provide such broad-band performance. On the other hand, the IF bandwidth is limited by the characteristics of the IF signal injected into the OSSBM device, that is, the amplitude and phase imbalance between the 90° hybrid outputs. However, one can expect bandwidths of 1–4 octaves even if one uses a commercially available 90° hybrid. This is an expected improvement from our previous scheme, where the IF bandwidth with a 20-dB IR ratio is restricted to only 20% of the IF frequency [8], [19].

Here, we discuss some limiting factors of the OE-IRM performance. The LR and IR ratios depend mainly on the optical carrier suppression and OLSB suppression ratios of the OSSBM device, respectively, which are primarily affected by the following factors: 1) accurate control in amplitudes, phases and bias of the OSSBM inputs and 2) its optical extinction ratio. However, high modulation indices of the MZM and OSSBM devices lead also to considerable increase of the third-order sidebands. The former corresponds to C and D in Fig. 2(a) and the latter to E in Fig. 2(b). For example, the LSB component is generated through the optical beat between the higher order sideband of the optical LO signal at $f_0 + 3f_{\rm LO}/2$ [D in Fig. 2(b)] and OUSB at $f_0 + f_{\rm LO}/2 + f_{\rm IF}$ [H in Fig. 2(b)], causing a possible degradation in the IR ratio. To prevent the degradation, the MZM modulation index should be kept moderate or the higher sideband [D in Fig. 2(b)] should be filtered out optically. Furthermore, the OSSBM modulation index should be adjusted in order to suppress a third-order sideband at $f_{\rm LO} - 3f_{\rm IF}$.

III. Performance Characterization and Fiber-Optic Transmission Experiment

We investigated the characteristics of the present OE-IRM scheme and its application capability to fiber-optic millimeter-wave links by using the experimental setup shown in Fig. 3. The OSSBM device is made of an x-cut $LiNbO_3$ crystal, whose detailed structure is described in [18]. There are two RF input ports (RFA and RFB) to which IF signals were applied

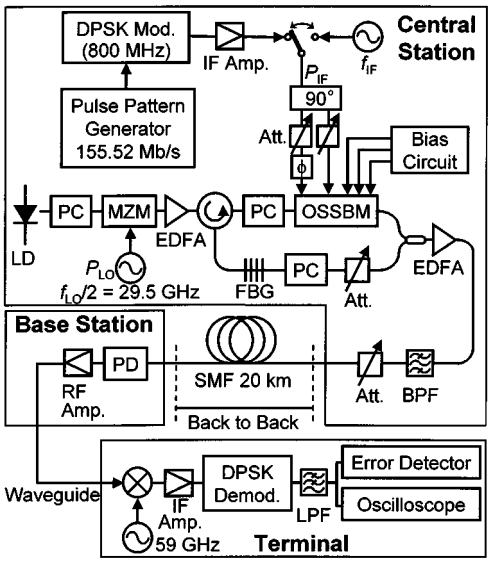

Fig. 3. Experimental setup.

with a phase difference of 90°. The half-wavelength voltages (V_π) of the OSSBM device are 6.0 V for RFA and 6.3 V for RFB at 100 MHz. V_π of the MZM device is 5.0 V at 29.5 GHz. To optimize the polarization states, we inserted optical polarization controllers at the OSSBM input and the FBG output. Erbium-doped amplifiers (EDFAs) were placed at the output ports of the MZM device and OE-IRM so as to compensate for the optical losses of MZM and OSSBM, which are typically 25.2 and 19.9 dB, respectively. The optical powers at the input ports of MZM and OSSBM are 6.0 and −2.6 dBm, respectively. An optical attenuator was used at the FBG output to adjust the power balance between the optical dual modes of OE-IRM output so that a high modulation index was provided. We used two kinds of IF signals in the experiments. One is a single tone signal coming from a synthesized signal generator and the other is a 155.52-Mb/s-DPSK 800-MHz signal. One of these IF signals was divided into two by a 90° hybrid whose operation band ranges from 500 to 1000 MHz, and their amplitudes and phases were trimmed before their injection into the OSSBM device. An optical bandpass filter having a 1.0-nm bandwidth was utilized to remove the ASE noise originating from EDFAs. The OE-IRM output light was launched into a 20-km SMF and transmitted to a BS. The details of the fiber-optic transmission experiment are described later. The following parameters are typical hereafter: $f_{\rm LO}$ is 59 GHz, the LO signal power at the MZM input is 6 dBm, $f_{\rm IF}$ is 800 MHz, and the IF signal power at the 90° hybrid input is 19 dBm, corresponding to the OSSBM input signal amplitudes of 1.39 V at RFA and 1.53 V at RFB. These values of RF power were chosen by taking their effects on the IR and TR ratios into consideration.

We have characterized the basic OE-IRM performance by using the single-tone IF signal. Fig. 4(a) and (b) shows the measured RF spectra at the PD output in the cases of back-to-back and 20-km SMF transmission, respectively. The IR and LR ratios are 46 and 28 dB, respectively, under the back-to-back condition. We also obtain a TR ratio of more than 36 dB, which originates from the third-order harmonic component not of OSSBM

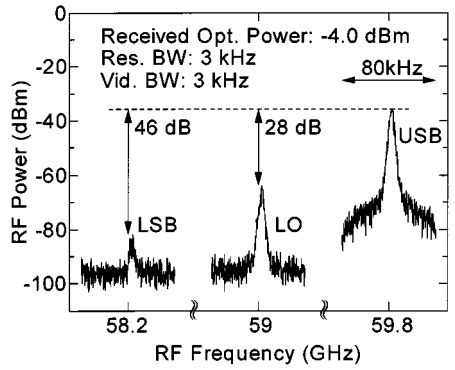

(a)

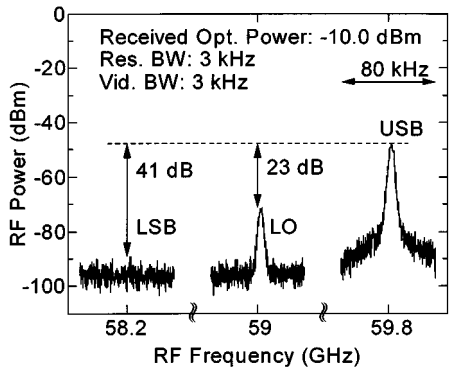

(b)

Fig. 4. RF spectra at the PD output without electrical amplification with a single-tone IF signal injected. LO and IF frequencies are 59 GHz and 800 MHz, respectively. (a) Under back-to-back conditions. (b) After 20-km SMF transmission.

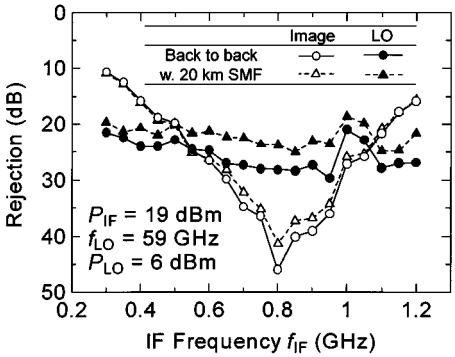

Fig. 5. Dependence of rejection ratios on IF frequency f_{IF}. The solid and dashed lines are guides for the eye.

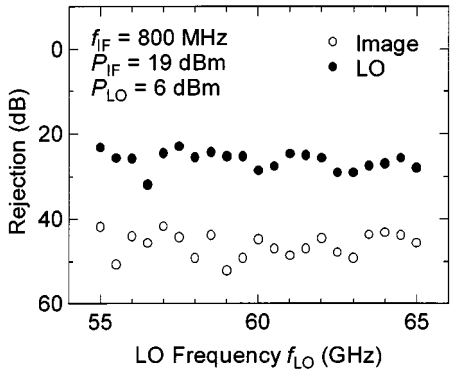

Fig. 6. Dependence of rejection ratios on LO frequency f_{LO}.

but of the IF signal of the synthesizer output. This is because the IF signal power was carefully suppressed so as to prevent the third-order nonlinearity of OSSBM. Hence, the TR ratio can be improved by appropriate filtering of the IF signal. We obtained an IR ratio of 41 dB and an LR ratio of 23 dB even after the 20-km transmission. The degradation in the IR ratio caused by the SMF transmission is not essential: the USB power was decreased by 12 dB because of the power loss induced in the transmission fiber (6 dB), while the LSB component fell below the noise floor of the spectrum analyzer. On the other hand, the LR ratio degradation can be ascribed to the residual carrier component at another polarization state generated in the present device.

The IR and LR ratios were measured as described in the following with various frequencies for IF and LO signals. The dependence of IR and LR ratios on f_{IF} is shown in Fig. 5. Even after the SMF transmission, an IR ratio of $>$20 dB was derived over an f_{IF} range from 550 to 1100 MHz, which corresponds to an IF bandwidth of 550 MHz, which we believe is limited by the 90° hybrid characteristics. The bandwidth will be broadened by using either hybrids of the multi-octave bandwidth or a higher IF frequency. LR ratios of $>$21 and $>$18.6 dB were confirmed in the f_{IF} range from 300 to 1200 MHz after and before the SMF transmission, respectively. The LR ratio achieves its minimum at $f_{\mathrm{IF}} = 1000$ MHz. The reason for this behavior has not been clarified yet. The LR degradation added through the fiber-optic transmission is 6.2 dB at most.

The dependence of IR and LR on the LO frequency f_{LO} is shown in Fig. 6. The measurements were restricted under the back-to-back condition for simplicity. Note that the IR ratio is more than 41 dB over the wide LO frequency range from 55 to 65 GHz, which is not limited by the configuration potential and can be extended to $2\delta f$ at most. However, the present acceptable bandwidth of LO frequency is approximately 16% of the LO frequency, which is still fairly large and superior to those of electrical IRMs. The LR ratio is $>$23 dB over the same LO frequency range.

We discuss the dependence of rejection ratios on power of LO and IF signals. The measured IR ratio degraded as the LO signal power exceeded 10 dBm, which is due to the increase of the higher order components of the optical LO signal [D in Fig. 2(b)]. The LSB component is thus generated through the beat note generation originating from the OSSBM output [H in Fig. 2(b)] and the increased D component. As for the measured TR ratio and its dependence on the IF signal power, they are dominated by the spurious component of the IF signal at present. However, it will be improved by appropriate IF filtering and is expected to be limited by the OSSBM third-order component. Based on the estimation of the third-order spurious of the OSSBM output, the limitation is given to be 45 dB at the IF signal power of 19 dBm.

Finally, we performed a preliminary fiber-optic transmission experiment of millimeter-wave signals using a 155.52-Mb/s-DPSK 800-MHz IF signal. A 59.8-GHz RF signal obtained through the photodetection was amplified and downconverted by a millimeter-wave mixer. In this experiment, the wireless transmission between the BS and the terminal was skipped for the sake of simplicity. The baseband signal was

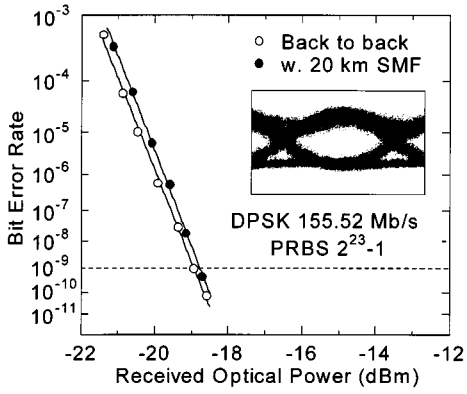

Fig. 7. BER characteristics and measured eye diagram at BER $= 10^{-9}$ (inset). IF frequency: 800 MHz; IF power: 19 dBm; LO frequency: 59 GHz; LO power: 6 dBm.

regenerated by the amplification and the DPSK demodulation. After the noise rejection by a 100-MHz lowpass filter, the obtained signal was injected into an error detector and an oscilloscope. The bit error rates (BERs) and the eye pattern thus derived are shown in Fig. 7. Clear eye opening was obtained and a BER of $<10^{-9}$ was achieved at the received optical power of -18 dBm. No floor was observed in the BER characteristics plotted as a function of the received optical power. In addition, the optical power penalty after the 20-km SMF transmission is as small as 0.2 dB, which indicates that the dispersion penalty is extremely suppressed. The applicability of the OE-IRM to fiber-optic millimeter-wave link was thus confirmed. We should note that its application to other modulation formats or subcarrier multiplexing is indispensable to clarify the features of the OE-IRM.

IV. Conclusion

We have implemented a 60-GHz optoelectronic image rejection mixer with an OSSBM device utilized and investigated its basic performance and application capability to millimeter-wave radio-on-fiber systems. Fairly high image and LO rejection ratios of >40 and >20 dB, respectively, have been achieved successfully. It has been clarified that the IF bandwidth of a 40-dB IR ratio is rather narrow but the IR ratio of >20 dB is provided over a bandwidth of 550 MHz, which is fairly broad considering the IF center frequency of 800 MHz. It is restricted by the bandwidth of the 90° hybrid we used in this particular experiment, and can be extended. Furthermore, it has been confirmed that the LO bandwidth of IR >40 dB is as broad as 10 GHz, which would be enough to cover the unlicensed millimeter-wave band, and is also expected to be broadened further. Notice that the last result is quite superior to that of electrical IRMs. In addition, the 155.52-Mb/s-DPSK 59.8-GHz optical millimeter-wave signal thus generated has been transmitted successfully over a 20-km SMF with a BER of $<10^{-9}$ at the optical received power of -18 dBm and scarce dispersion penalty (<0.2 dB). We believe that the OSSBM-based OE-IRM is of fairly high performance and will be useful in future millimeter-wave fiber radio systems.

Acknowledgment

The authors would like to thank Dr. M. Izutsu, Communications Research Laboratory, Tokyo, Japan, for his helpful discussions and encouragement and Dr. K. Kubodera, Sumitomo Osaka Cement, Osaka, Japan, for his kind support. The authors would also thank Dr. S. Shiraishi, Sumitomo Electric Industries, Chiba, Japan, and Dr. H. Hasebe, Sumitomo Electric Industries, Chiba, Japan, for providing the FBG.

References

[1] H. Ogawa, D. Polifko, and S. Banba, "Millimeter-wave fiber optics systems for personal radio communication," *IEEE Trans. Microwave Theory Tech.*, vol. 40, pp. 2285–2293, Dec. 1992.

[2] T. Kuri, K. Kitayama, A. Stöhr, and Y. Ogawa, "Fiber-optic millimeter-wave downlink system using 60 GHz-band external modulation," *J. Lightwave Technol.*, vol. 17, pp. 799–806, May 1999.

[3] G. H. Smith and D. Novak, "Broad-band millimeter-wave (38 GHz) fiber-wireless transmission system using electrical and optical SSB modulation to overcome dispersion effects," *IEEE Photon. Technol. Lett.*, vol. 10, pp. 141–143, 1998.

[4] T. Tanuma, "Millimeter-wave utilization and management in Japan," in *3rd Topical Millimeter Waves Symp. Tech. Dig.*, 2001, pp. 17–20.

[5] R. Hofstetter, H. Schmuck, and R. Heidemann, "Dispersion effects in optical millimeter-wave systems using self-heterodyne method for transport and generation," *IEEE Trans. Microwave Theory Tech.*, vol. 43, pp. 2263–2269, Sept. 1995.

[6] J. Park, M. S. Shakouri, and K. Y. Lau, "Millimeter-wave electro-optical upconverter for wireless digital communications," *Electron. Lett.*, vol. 31, pp. 1085–1086, 1995.

[7] K. Nishikawa and M. Tsuchiya, "60 GHz optoelectronic mixing with high image rejection ratio (>36dB)," in *Int. Microwave Photon. Topical Meeting Tech. Dig.*, 1999, F-9.5, pp. 235–238.

[8] Y. Ozeki, K. Nishikawa, M. Kishi, and M. Tsuchiya, "60 GHz optoelectronic image rejection mixer and its application to a 156 Mb/s fiber-optic MM-wave link," *IEEE Photon. Technol. Lett.*, vol. 13, pp. 361–363, Apr. 2001.

[9] M. Izutsu, S. Shikama, and T. Sueta, "Integrated optical SSB modulator/frequency shifter," *IEEE J. Quantum Electron.*, vol. QE-17, pp. 2225–2227, 1981.

[10] S. Shimotsu, S. Oikawa, T. Saitou, N. Mitsugi, K. Kubodera, T. Kawanishi, and M. Izutsu, "Single side-band modulation performance of a $LiNbO_3$ integrated modulator consisting of four-phase modulator waveguides," *IEEE Photon. Technol. Lett.*, vol. 13, pp. 364–366, Apr. 2001.

[11] P. Suwonpanich, K. Tsukamoto, and S. Komaki, "Proposal of radio-over-fiber systems using cascaded radio-to-optic direct conversion scheme," *IEICE Trans. Commun.*, vol. E83-B, pp. 1766–1774, 2000.

[12] J. J. O'Reilly, P. M. Lane, R. Heidemann, and R. Hofstetter, "Optical generation of very narrow linewidth millimeter wave signals," *Electron. Lett.*, vol. 28, pp. 2309–2311, 1992.

[13] D. Wake, C. R. Lima, and P. A. Davies, "Transmission of 60-GHz signals over 100 km of optical fiber using a dual-mode semiconductor laser source," *IEEE Photon. Technol. Lett.*, vol. 8, pp. 578–580, 1996.

[14] L. Noël, D. Wake, D. G. Moodie, D. D. Marcenac, L. D. Westbrook, and D. Nesset, "Novel techniques for high-capacity 60-GHz fiber-radio transmission systems," *IEEE Trans. Microwave Theory Tech.*, vol. 45, pp. 1416–1423, Aug. 1997.

[15] K. Sato, A. Hirano, N. Shimizu, T. Ohno, and H. Ishii, "Optical millimeter-wave generation by dual-mode operation of semiconductor modelocked lasers," *Electron. Lett.*, vol. 36, pp. 340–341, 2000.

[16] U. Gliese, S. Nørskov, and T. N. Nielsen, "Chromatic dispersion in fiber-optic microwave and millimeter-wave links," *IEEE Trans. Microwave Theory Tech.*, vol. 44, pp. 1716–1724, Oct. 1996.

[17] S. Shimotsu, M. Izutsu, T. Kawanishi, S. Oikawa, and M. Sasaki, "Wide-band frequency conversion with $LiNbO_3$ optical single-sideband modulator," in *OFC2001 Tech. Dig.*, 2001, WK3.

[18] K. Higuma, S. Oikawa, Y. Hashimoto, H. Nagata, and M. Izutsu, "X-cut lithium niobate optical single-sideband modulator," *Electron. Lett.*, vol. 37, pp. 515–516, 2001.

[19] Y. Ozeki, K. Nishikawa, M. Kishi, and M. Tsuchiya, "156 Mb/s DPSK optical MM-wave transmission employing a 60 GHz optoelectronic image rejection mixer," in *Int. Microwave Photon. Topical Meeting Tech. Dig.*, 2000, WE1.4, pp. 137–140.

Yasuyuki Ozeki (S'99) was born in Mie, Japan, on February 8, 1977. He received the B.S. and M.S. degrees in electronic engineering from the University of Tokyo, Tokyo, Japan, in 1999 and 2001, respectively, and is currently working toward the Ph.D. degree at the the University of Tokyo.

His research focuses on millimeter-wave photonics.

Mr. Ozeki is a member of the Institute of Electronics, Information and Communication Engineers (IEICE), Japan.

Kaoru Higuma received the B.S. degree in physics and the M.E. degree in applied optics from Waseda University, Tokyo, Japan, in 1994 and 1996, respectively.

In 1996, he joined Sumitomo Osaka Cement, Chiba, Japan, where he has been engaged in the research and development of optical $LiNbO_3$ modulators.

Satoshi Oikawa received the B.E. and M.E. degrees in electrical engineering from Nihon University, Tokyo, Japan, in 1991 and 1993, respectively.

In 1993, he joined the Optoelctronics Research Division, New Technology Research Laboratories, Sumitomo Osaka Cement, Chiba, Japan, where he has been engaged in the research and development of optical $LiNbO_3$ modulators.

Masato Kishi was born in Tokyo, Japan. He received the B.S. and M.S. degrees in physics from Nihon University, Tokyo, Japan, in 1972 and 1974, respectively.

In 1990, he joined the Department of Electrical Engineering, University of Tokyo, Tokyo, Japan, where he is currently a Research Associate. He has been involved in the study of material science.

Masahiro Tsuchiya (M'97) was born in Shizuoka, Japan, on September 28, 1960. He received the B.S., M.S., and Ph.D. degrees from the University of Tokyo, Tokyo, Japan, in 1983, 1985, and 1988, respectively, all in electronic engineering. His doctoral dissertation concerned resonant tunneling devices and phenomena in ultrathin semiconductor hetero-structures.

From 1988 to 1990, he was a Post-Doctoral Fellow with the University of California at Santa Barbara, where he was engaged in studies on quantum microstructures and their applications to optoelectronic devices. In 1990, he joined the Research Development Corporation of Japan (JRDC), where he dealt with researches of quantum devices with emphasis on FETs containing coupled quantum wells and quantum wires. In 1991, he became a Lecturer in the Department of Electronic Engineering, University of Tokyo, and in 1993, was appointed an Associate Professor in the same department. In 1996, he spent his sabbatical year as a Visiting Researcher at Bell Laboratories, AT&T, and Lucent Technologies, Holmdel, NJ. His current interests are ultrafast optoelectronics, millimeter-wave photonics, optical probing techniques for high-frequency circuit diagnosis, and Raman spectroscopy.

Dr. Tsuchiya is a member of the IEEE Lasers and Electro-Optics Society (IEEE LEOS), the Japan Society of Applied Physics, and the Institute of Electronic, Information and Communication Engineers (IEICE), Japan.